

FUZZY BASED OPTIMAL NETWORK RECONFIGURATION OF DISTRIBUTION SYSTEM WITH ELECTRIC VEHICLE CHARGING STATIONS, DISTRIBUTED GENERATION, AND SHUNT CAPACITORS

Ajit Kumar MOHANTY , Suresh Babu PERLI 

Department of Electrical Engineering, National Institute of Technology, Warangal,
National Institute of Technology Campus, Hanamkonda, 506004 Telengana, India

ajitchinu@student.nitw.ac.in, drsureshperli@nitw.ac.in

DOI: 10.15598/aece.v21i2.4599

Article history: Received Jun 15, 2022; Revised Sep 18, 2022; Accepted May 11, 2023; Published Jun 30, 2023.
This is an open access article under the BY-CC license.

Abstract. Electric Vehicles (EVs) are gaining popularity due to their low maintenance, better performance and zero carbon emission. To expand their adoption, Electric Vehicles Charging Stations (EVCS) must be integrated with the distribution system constructively to charge EVs. This study suggests an RAO-3 based on the fuzzy classification technique for the optimum EVCS, Distributed Generations (DGs), and Shunt Capacitors (SCs) sizing and positioning for 69 bus radial distribution systems with network reconfiguration. The proposed method has the following advantages (i) lower active power loss, (ii) enhanced voltage profiles, (iii) improved power factor at the substation, and (iv) optimum distribution of EVs at charging stations. Characteristic curves of Li-Ion battery charging are utilised for load flow analysis to build EV battery charging loads models. The proposed simultaneous fuzzy multi-objective study with a reconfigured network can handle the optimal number of EVs in EVCS and maintain the substation power factor at the required level, yielding an impressive distribution system performance. For example, the minimum active power loss of 18.0884 kW is achieved with a minimum voltage enhanced to 0.9905 p.u., maintaining the bus voltages at their permissible limit. The numerical results indicate that using the RAO-3 algorithm, the simultaneous technique with system reconfiguration is computationally efficient and scalable, outperforming the two-stage methodology and the method without system reconfiguration.

Keywords

Distributed Generators, Electric Vehicles, Electric Vehicle Charging Stations, Substation.

1. Introduction

The rapid adoption of EVs in transportation in place of conventional commercial vehicles can help to minimise air pollution and fossil fuel dependency. The EVCS must be integrated with distribution networks to reduce losses and increase voltage stability [1]. In order to minimise this problem, this paper includes network reconfiguration, DGs, and SCs placement.

Electrical harmonics, poor power factor, voltage instability, and imbalance are all randomly caused by the integration of EVCS into the existing grid infrastructure [2] and [3]. Many elements [4] influence the distribution system, including charging techniques, vehicle density at charging stations, etc. Experimental studies [5] and [6] are used to examine and validate the impact of EVCS on the distribution network with the objective function of initial investment cost and power quality factors. The influence of EVCS on a distributed system is investigated [7], [8] and [9] in the evolution of the power grid moving towards sustainable energy, with EVs affecting and supporting future energy growth.

The impact of EVCS on the distribution system is mitigated by network reconfiguration. The distribution network's power loss will not be minimal with variable

load demand and fixed network topology. As a result, timely network reconfiguration is essential. In order to relieve overcrowded feeders and reduce real power loss in the distribution system, network reconfiguration is generally favoured [10] and [11].

On the other hand, reconfiguring the network may not meet the desired power loss reduction and power quality limitations. As a result, network reconfiguration is used in conjunction with Shunt Capacitors (SCs) or Distributed Generators (DGs) to improve voltage profile and minimise power losses and energy savings [12], [13], [14], [15] and [16]. The author of [17] developed a two-stage process for determining the best location for EVCS, DGs, and SCs. DGs and SCs are optimally situated in the initial stage. EVs are installed later in the second stage. This author does not examine the substation power factor after the installation of EVCS.

Various optimisation problems can be solved using the metaheuristic technique. In [18] used a PSO method to allocate EVs in the given system. In the literature [19] and [20] JAYA and Grey Wolf Optimizer algorithms are used to integrate EVCS in the distribution systems. In this paper a robust optimisation technique known as Rao algorithms [21] is used to tackle the proposed problem. The effect of EV battery charging rates on the distribution system's performance are investigated [22] and [23].

Most of the literature review discusses appropriate EVCS allocation in distribution systems without considering substation power factor. In this study, the electrical distribution network is reconfigured, and optimal simultaneous EVCS, DGs, and SCs are placed with a fuzzy multi-objective approach based on the RAO-3 algorithm for better distribution network performance, such as reducing active power loss, enhancing voltage profile, and keeping Substation (SN) pf at the optimal value. The performance of the RAO-3 algorithm is compared with conventional algorithms like Particle Swarm Optimisation (PSO), Artificial Bee Colony (ABC), and Grey Wolf Optimiser (GWO).

This work's main points can be summed up as follows:

1. The distribution network's EVCS, DGs, and SCs are all sized and placed optimally simultaneously with the optimal quantity of EVs.
2. In the distribution network reconfiguration, simultaneous optimal sizing and position of EVCS, DGs, and SCs with the optimal quantity of EVs.
3. In order to investigate the effect of EVCS on the distribution system's performance, EV battery charging loads models are developed.

The rest of the paper is organised in the following manner: Sec. 2. discusses the fuzzy multi-objective formulation of the problem and its constraints. Section 3. discusses the fuzzy multi-objective RAO technique. Section 4. includes the results and analyses, whereas Sec. 5. has the conclusions.

2. Problem Formulation

The fuzzy-based multi-objective functions necessary for optimal deployment of EVCS, DGs, and SCs in order to improve distribution system performance are established in this section.

2.1. Substation Power Factor Membership Function:

The DGs primarily run at 0.95 lagging pf ; hence, the goal is to improve the Substation (SN) pf to 0.95 lagging. The following equation can be used to compute the substation power factor.

$$pf = \cos \left(\frac{S_{kW}^{SN}}{S_{kVA}^{SN}} \right), \quad (1)$$

$$S_{kW}^{SN} = \sum_{m=1}^{nbs} P_m^{load} + Pl - \sum_{n=1}^{ndg} P_n^{DG}, \quad (2)$$

$$S_{kVAr}^{SN} = \sum_{m=1}^{nbs} Q_m^{load} + Ql - \sum_{o=1}^{nsc} Q_o^{SC} - \sum_{n=1}^{ndg} P_n^{DG} \times \emptyset_{dg}, \quad (3)$$

$$S_{kVA}^{SN} = \sqrt{S_{kW}^{SN2} + S_{kVAr}^{SN2}}. \quad (4)$$

S_{kW}^{SN} and S_{kVA}^{SN} are the active and reactive power drawn from the substation. P_n^{DG} is the capacity of the nth DG. The total no-of DGs installations is ndg . \emptyset_{dg} is the DGs units' power factor angle. The m^{th} node's active power and reactive power loads are P_m^{load} and Q_m^{load} .

nbs is the total number of buses in the distribution network. Pl is the real power loss and Ql is the reactive power loss of the distribution system. The capacity rating of shunt reactive is Q_o^{SC} . The total number of SCs installations is nsc . The fuzzy membership function for the SN Power-Factor (pf) [17] is depicted in Fig. (1(a)), and the mathematical expression is given in Eq. (5).

$$\delta^{pf} = \begin{cases} 0 & \text{for } pf \leq pf_{\min}, \\ \frac{pf - pf_{\min}}{pf_s - pf_{\min}} & \text{for } pf_{\min} \leq pf \leq pf_s, \\ \frac{pf_{\max} - pf}{pf_{\max} - pf_s} & \text{for } pf_s \leq pf \leq pf_{\max}, \\ 0 & \text{for } pf \geq pf_{\max}, \end{cases} \quad (5)$$

$pf_{\min} = 0.85$, $pf_s = 0.95$, $pf_{\max} = 1$ are assumed.

2.2. DGs Penetration Membership Function:

The DGP is the proportion of installed DGs to total active power load.

$$DGP = \frac{\sum_{n=1}^{ndg} P_n^{DG}}{\sum_{m=1}^{nbs} P_{load}^m}, \quad (6)$$

The fuzzy membership function for the DGs penetration [17] is shown in Fig.1(b) and mathematical expression is given in equation Eq. (7).

$$\delta^{DGP} = \begin{cases} 0 & \text{for } DGP \leq DGP_{\min}, \\ \frac{DGP - DGP_{\min}}{DGP_s - DGP_{\min}} & \text{for } DGP_{\min} \leq DGP \leq DGP_s, \\ \frac{DGP_{\max} - DGP}{DGP_{\max} - DGP_s} & \text{for } DGP_s \leq DGP \leq DGP_{\max}, \\ 0 & \text{for } DGP \geq DGP_{\max}, \end{cases} \quad (7)$$

$DGP_{\min} = 0.4$, $DGP_s = 0.5$, $DGP_{\max} = 0.6$ respectively. DGP_s is the desired penetration level in the distribution system. Percentage penetration is believed to be 50 % in this work.

2.3. Active Power Loss Membership Function:

The following equation depicts the distribution network's Active power Loss (AL):

$$AL = \sum_{m=1}^{nbs-1} Pl_m, \quad (8)$$

Pl_m represents the branch active power loss [25], where formulated from the following equation:

$$Pl_m = \frac{r_m \times \{P_{m+1}^2 + Q_{m+1}^2\}}{|v_{m+1}|^2}, \quad (9)$$

where P_{m+1} is the active power load injected at the load ($m + 1$) node and Q_{m+1} is the reactive power load.

The following formula can be used to determine the active power loss index (ALX):

$$ALX = \frac{AL_{DGSC}}{AL_{Base}}, \quad (10)$$

With DGs and SCs, AL_{DGSC} denotes active power loss. AL_{Base} denotes the real power loss in the base case. The fuzzy membership function for the real power loss [17] is depicted in Fig. 1(c) and mathematical expression is given in equation Eq. (11). $ALX^{\max} = 1$. ALX^{\min} is chosen based on utility necessity so that active power loss is minimized to a desirable value.

$$\delta^{ALX} = \begin{cases} 1 & \text{for } ALX \leq ALX^{\min}, \\ \frac{ALX^{\max} - ALX}{ALX^{\max} - ALX^{\min}} & \text{for } ALX^{\min} \leq ALX \leq ALX^{\max}, \\ 0 & \text{for } ALX > ALX^{\max}. \end{cases} \quad (11)$$

2.4. Distribution System Voltage Membership Function:

In Fig. 1(d), the fuzzy membership function of voltage [17] (δ^{v_m}) of each node m in the distribution system is explained, and it can be mathematically explained using Eq. (12). $v_{ld1} = 0.94$, $v_{\min} = 0.95$, $v_{\max} = 1.05$, $v_{ld2} = 1.06$ are assumed. The distribution system's fuzzy voltage limit is now defined as $\delta^v = \min(\delta^{v_m})$:

$$\delta^{v_m} = \begin{cases} 0 & \text{for } v_m \leq v_{ld1}, \\ \frac{v_m - v_{ld1}}{v_{\min} - v_{ld1}} & \text{for } v_{ld1} < v_m < v_{\min}, \\ 1 & \text{for } v_{\min} \leq v_m \leq v_{\max}, \\ \frac{v_m - v_{\max}}{v_{ld2} - v_{\max}} & \text{for } v_{\max} < v_j < v_{ld2}, \\ 0 & \text{for } v_m > v_{ld2}. \end{cases} \quad (12)$$

2.5. Reconfiguration Methodology

To determine the efficacy of loss reduction, the researchers' proposed optimum network reconfiguration switching strategies must consider each feasible transition. In [11] the proposed network reconfiguration strategy is described in detail.

2.6. Optimal Allocations of EVs, DGs, and SCs Using a Multi-objective Fuzzy Function:

$$G_{zs} = \frac{1}{\delta^{ALX} + \delta^{pf} + \delta^v + \delta^{DGP}}. \quad (13)$$

The propose method is to minimise fuzzy function described in equation Eq. (13), which is exposed to various constraints:

$$0 < P_n^{DG} \leq P_{\max}^{DG}, \text{ where } n = 1, 2, 3, \quad (14)$$

$$0 < Q_o^{sc} \leq Q_{\max}^{sc}, \text{ where } o = 1, 2, 3. \quad (15)$$

The DGs and SCs power injection at the optimal point in the distribution system are P_n^{DG} and Q_o^{sc} .

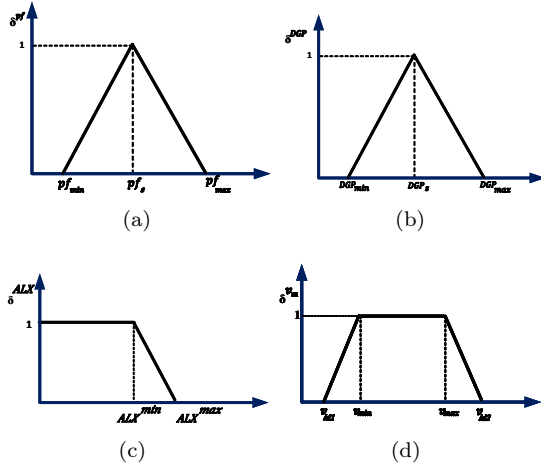


Fig. 1: Fuzzy membership function.

2.7. Battery Charging Load Modelling for EVs:

Equations for load flow analysis using the battery charging load model [22] can be generated from Fig. (2). Eq. (16) depicts the charging of a battery for both steady-state and transient circumstances. The following exponential equations can be used to predict the power charging properties of batteries [17]:

$$P_{BEV}(t) = \begin{cases} P_{BEV}^{\max} \left(1 - e^{\left(\frac{-\gamma \times t}{t_2}\right)} \right), & 0 \leq t \leq t_2, \\ P_{BEV}^{\max} \left(\frac{t_m - t}{t_m - t_2} \right), & t_2 \leq t \leq t_m, \\ 0, & t > t_m. \end{cases} \quad (16)$$

The instantaneous electric vehicle battery charging load is $P_{BEV}(t)$. P_{BEV}^{\max} is the substation's maximum battery charging load.

$$\delta P_{BEV}^{\max} = P_{BEV}^{\max} \left(1 - e^{\left(\frac{-\gamma \times t_1}{t_2}\right)} \right), \quad (17)$$

$$\gamma = - \left(\frac{t_2}{t_1} \right) \ln(1 - \delta), \quad (18)$$

$t_1 = 0.25$ h, $t_2 = 4.5$ h, and $t_m = 5$ h are in the preceding Eq. (16) and Eq. (17), respectively, taken from Fig. 2. The EV battery characteristic constants are γ and δ . δ is the proportion of maximum load for charging, with a value of 0.95 corresponding to 95 % of P_{BEV}^{\max} at time t_1 . Eq. (18) (which may be derived from Eq. (17)) can be used to find the value of γ . The equation for power charging can be represented as Eq. (19). The batteries are charged from a zero-charge condition P_{BEV}^0 .

$$P_{BEV}(t) = P_{BEV}^{\max} \left(1 - e^{\left(\frac{-\gamma \times t}{t_c}\right)} \right) + P_{BEV}^0 \left(e^{\left(\frac{-\gamma \times t}{t_c}\right)} \right), \quad (19) \quad 0 < t < t_c.$$

The t_c represents the amount of time it takes to charge a battery from its starting charging position fully. The following equation can be used to represent the status of the power charging battery.

$$SOC(t+1) = SOC(t) + P_{BEV}(t) \times \Delta(t). \quad (20)$$

3. RAO-3 Algorithm

RAO-3 and RAO-1 are new optimisation algorithms [21]. It was chosen as a population-based approach for this study because of its simplicity and ease of implementation in optimization applications. It has a few control parameters. The population size is the sole control parameter that must be changed once the stop criteria are met. The proposed RAO-3 and RAO-1 algorithms make use of the worst and best solutions that can be found in Eq. (21) and Eq. (22):

$$y'_{m,p,i} = y_{m,p,i} + rand_{1,m,i} \times (y_{m,b,i} - |y_{m,w,i}|) + rand_{2,m,i} \times (|y_{m,p,i} \text{ or } y_{m,d,i}| - (y_{m,d,i} \text{ or } y_{m,p,i})), \quad (21)$$

$$y'_{m,p,i} = y_{m,p,i} + rand_{1,m,i} \times (y_{m,b,i} - y_{m,w,i}), \quad (22)$$

$y_{m,p,i}$ is the m^{th} variable's value for the p^{th} candidate in the i^{th} iteration. The best candidate solution is denoted by $y_{m,b,i}$, whereas the worst candidate solution is denoted by $y_{m,w,i}$.

Between exploitation and exploration, the Rao-3 algorithm can ensure optimum equilibrium. Figure 3 illustrates the suggested approach and is thoroughly explained in the steps that follow:

- Step 1: Read Distribution system data and run the load flow for the base case.
- Step 2: Initialise the algorithm parameters such as population, dimension (location and size), iteration (itr), and the maximum number of iterations (itrmax).
- Step 3: Randomly initialise the EVCS, DGs, and SCs location and sizes within maximum and minimum limits.
- Step 4: Run the load flow. Determine the fitness values for every population using Eq. (5), Eq. (6), Eq. (7), Eq. (8), Eq. (9), Eq. (10), Eq. (11), Eq. (12) and Eq. (13).
- Step 5: Determine the population's best and worst solutions.
- Step 6: The objective function values are selected to provide the optimal solution, which is then compared to the previous one. If the

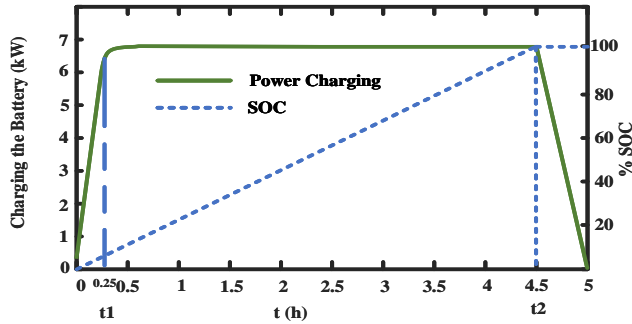


Fig. 2: Li-Ion battery charging characteristics.

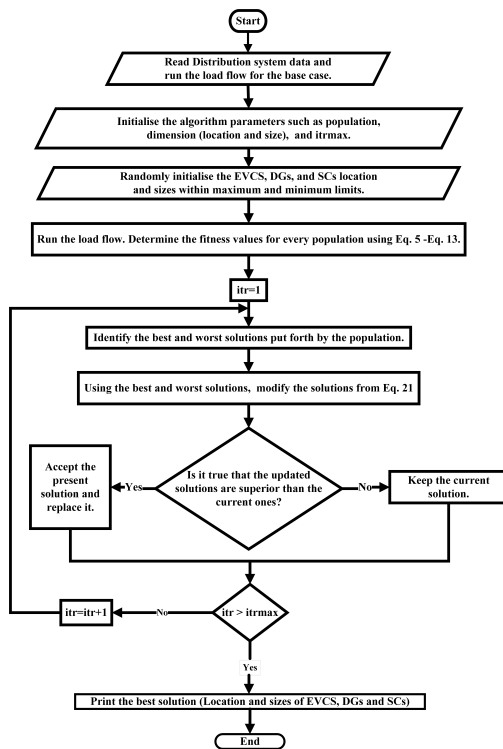


Fig. 3: RAO-3 flow chart for the placement of EVCS, DGs, and SCs.

new solution is superior to the previous one, the previous one will be replaced.

Step 7: Whether the criterion is not satisfied, proceed to Step 5; otherwise, display the best optimal solution.

4. Result and Discussions

In this study, a 69 bus radial distribution system [24], three bus nodes of DGs units, three bus nodes of SCs units and five EVCS bus nodes are considered. In the algorithm, parameters such as population = 100 and itrmax = 100 are assumed. Furthermore, maximum 50 EVs can be charged at each charging station are

assumed. A Li-Ion battery’s maximum charging load during steady charge is 6.5 kW, according to the characteristic charging curve depicted in Fig. 2. The given system’s base values are 100 MVA and 12.66 kV. In the base case based on load flow following data, the active power demand is 3082.19 kW, the reactive power demand is 2796.77 kVAr, total real power loss is 225 kW, and the lowest voltage is 0.9092 p.u. The proposed problem is solved using the MATLAB 2022 a software installed with an Intel Core i5 8th Gen processor and 8 GB RAM.

Two scenarios are studied for EVCS, DGs, and SCs in a particular distribution network to be sized and placed optimally:

4.1. Scenario 1

Fuzzy multi-objective functions described in this paper’s Eq. (13) are placed optimally using the RAO-3 method by DGs, SCs, and EVCS.

The total power loss of the distribution network has decreased to 39.3467 kW and the minimum voltage was improved to 0.9762 p.u. The optimal number of EVs that can accommodate at EVCS is 193. The optimal number of EVs and EVCS are depicted in Tab. 1. Table 2 and Tab. 3 shows the DGs and SCs optimal location and size. Table 4 shows the distribution system’s performance. Figure 4 and Fig. 5 illustrate the fitness function and voltage profile curves, respectively. Figure 6 shows a single line diagram of the 69 bus radial distribution system with EVCS, DGs, and SCs from scenario 1.

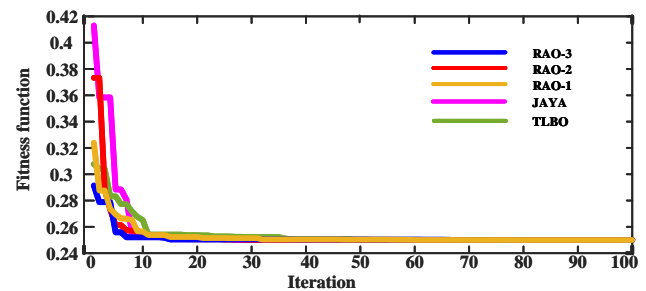


Fig. 4: Simultaneous placement of EVCS, DGs, and SCs fitness curve.

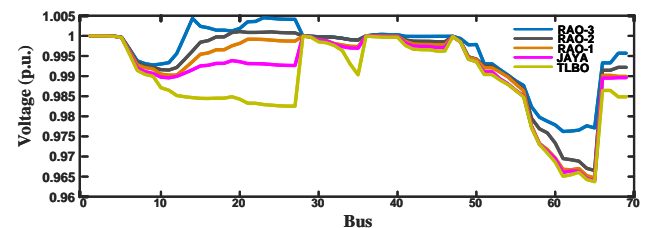


Fig. 5: Simultaneous placement of EVCS, DGs, and SCs Volt- age curve.

Tab. 1: Optimum number of EVs and optimum location of EVCS.

Fuzzy PSO		Fuzzy ABC		Fuzzy GWO		Fuzzy RAO-1		Fuzzy RAO-3	
Optimum node for EVs locations	Optimum no-of EVs	Optimum node for EVs locations	Optimum no-of EVs	Optimum node for EVs locations	Optimum no-of EVs	Optimum node for EVs locations	Optimum no-of EVs	Optimum node for EVs locations	Optimum no-of EVs
31	24	48	34	10	31	53	38	6	38
19	38	9	41	40	35	56	37	18	45
48	32	45	33	36	36	3	33	30	35
43	31	47	36	45	36	37	50	60	30
32	42	18	33	35	43	39	30	40	45
Total no-of EVs	167	Total no-of EVs	177	Total no-of EVs	181	Total no-of EVs	188	Total no-of EVs	193

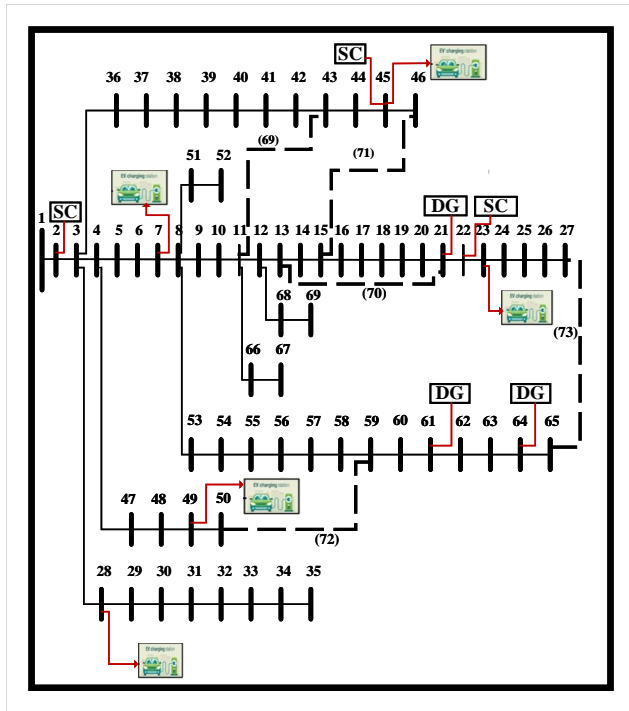


Fig. 6: 69 bus radial distribution system with EVCS, DGs and SCs.

4.2. Scenario 2

In this scenario, first network reconfiguration of 69 bus radial system is done. The system’s real-power loss prior to reconfiguration was 224.95 kW, and the lowest system voltage $V_{min}=0.9092$ p.u.

After network reconfiguration, the active power loss of 69 bus radial distribution network was reduced to 98.5512 kW, i.e., 56.1789 % power loss reduction, and minimum voltage is increased to $V_{min} = 0.94947$ p.u. which is shown in Fig. 7. Table 5 represents the performances of distribution system after network reconfiguration.

DGs, SCs, and EVCS are optimally positioned in the distribution system obtained from network reconfiguration. In this scenario, the distribution system’s overall power loss was decreased to 18.0884 kW and minimum voltage improves to 0.9905 p.u. The optimal number of EVs has been increased to 213 vehicles. Table 6 shows

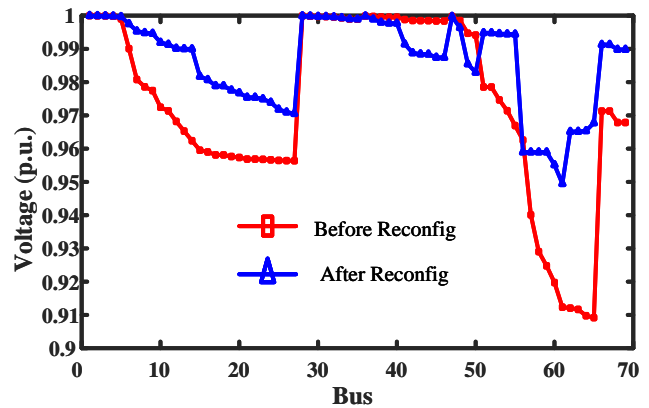


Fig. 7: Voltage curve before and after reconfiguration.

the performance of the distribution system, the optimal location and sizing of DGs and SCs are illustrated in Tab. 7 and Tab. 8. Table. 9 examines the distribution system’s performance. Based on the performance, RAO-3 algorithm outperforms the other conventional algorithm. Figure 8 and Fig. 9 depicts the fitness function and voltage profile curves, respectively. Figure 10 shows a single line diagram of the after-network reconfiguration of the 69 bus radial distribution system with EVCS, DGs, and SCs from scenario 2.

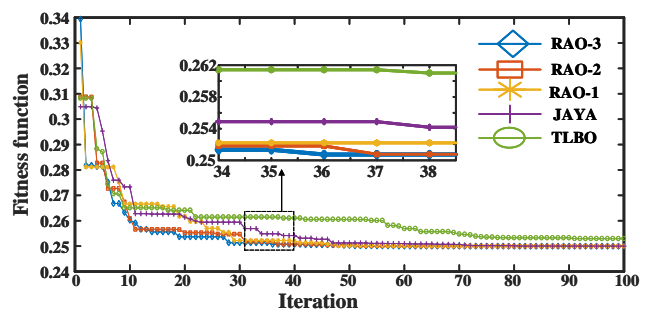


Fig. 8: Fitness curve.

According to the previous findings, scenario 2 performs better than the other scenario. Table 10 compares the outcomes of all of the scenarios.

Compared to the base case, two-stage methodology [17], and scenario 1, the active power loss in scenario 2 is reduced to 91.9589 %, 55.89 %, and 54.028 %. Compared to the base case minimum voltage of 0.9092, the

Tab. 2: DGs optimum location and sizing.

Fuzzy PSO		Fuzzy ABC		Fuzzy GWO		Fuzzy RAO-1		Fuzzy RAO-3	
DG Node location	DG sizing (kW)								
63	900	19	529.4247	61	898.3838	61	806.9187	13	507.8488
23	900	61	871.2734	14	900.0000	59	591.6334	21	539.3180
6	100.7	10	500.0016	24	102.3163	19	502.1479	61	853.5330

Tab. 3: SCs optimum location and sizing.

Fuzzy PSO		Fuzzy ABC		Fuzzy GWO		Fuzzy RAO-1		Fuzzy RAO-3	
SC Node location	SC sizing (kVAr)								
38	540.1420	32	457.3101	38	575.9351	50	511.6601	64	595.8269
58	582.9905	62	472.1094	62	519.4239	40	241.6474	69	372.0686
69	241.5578	28	455.2351	69	266.6933	12	635.2496	22	392.8228

Tab. 4: 69 bus system performance comparison.

69 bus	Base case	Fuzzy PSO	Fuzzy ABC	Fuzzy GWO	Fuzzy RAO-1	Fuzzy RAO-3
SN real power (kW)	4027.19	2240.19	2223.76	2218.69	2173.09	2131.49
SN Reactive power (kVAr)	2796.77	733.7	731.01	719.2853	710.0001	702.53
SN pf	0.8214	0.95 lag	0.95 lag	0.95 lag	0.95 lag	0.95 lag
DGs Penetration	-	1900.7	1900.7	1900.7	1900.7	1900.7
Real Power loss (kW)	224.95	45.1027	43.9481	43.7336	41.688	39.3467
Voltage minimum (p.u.)	0.9092	0.96507	0.96605	0.96681	0.96948	0.9762

Tab. 5: Performances of distribution system after network reconfiguration.

Entity	Base case	Fuzzy PSO	Fuzzy ABC	Fuzzy GWO	Fuzzy RAO-1	Fuzzy RAO-3
Tie Switches	69, 70, 71, 72, 73	17, 55, 61, 69, 71	9, 17, 56, 63, 71	14, 57, 61, 69, 70	14, 57, 61, 69, 70	14, 55, 61, 69, 70
Active Power loss (kW)	224.95	115.7826	112.8772	98.6046	98.6046	98.5512
$V_{min}(p.u.)$	0.9092	0.94831	0.94831	0.94947	0.94947	0.94947

Tab. 6: Performance comparison of 69 bus system.

69 bus	Base case	Fuzzy PSO	Fuzzy ABC	Fuzzy GWO	Fuzzy RAO-1	Fuzzy RAO-3
SN Active power (kW)	4027.19	3053.60	3154.76	3155.33	3257.9	3303.3
SN Reactive power (kVAr)	2796.77	1003.673	1036.919	1037.106	1070.8	1085.71
SN pf	0.8214	0.95 lag	0.95 lag	0.95 lag	0.95 lag	0.95 lag
DGs Penetration	-	1900.4177	1900.5	1900.6997	1900.70727	1901.69996
Real Power loss (kW)	224.95	20.06	19.64	19.09	18.2453	18.0884
Voltage minimum (p.u.)	0.9092	0.9811	0.9812	0.9852	0.9868	0.9905

Tab. 7: Optimum number of EVs and optimum location of EVCS.

Fuzzy PSO		Fuzzy ABC		Fuzzy GWO		Fuzzy RAO-1		Fuzzy RAO-3	
Optimum node for EVs locations	Optimum no-of EVs	Optimum node for EVs locations	Optimum no-of EVs	Optimum node for EVs locations	Optimum no-of EVs	Optimum node for EVs locations	Optimum no-of EVs	Optimum node for EVs locations	Optimum no-of EVs
19	36	28	36	31	38	39	39	42	46
42	35	44	39	38	39	38	41	27	38
36	44	30	36	28	34	37	44	32	45
38	40	47	39	37	44	28	39	7	48
48	35	25	40	35	35	36	43	58	36
Total no-of EVs	190	Total no-of EVs	190	Total no-of EVs	190	Total no-of EVs	206	Total no-of EVs	213

Tab. 8: DGs optimum location and sizing.

Fuzzy PSO		Fuzzy ABC		Fuzzy GWO		Fuzzy RAO-1		Fuzzy RAO-3	
DG Node location	DG sizing (kW)								
61	812.6740	23	591.1429	21	535.7574	57	373.9585	61	885.1275
27	574.4756	61	850.1275	60	513.8592	61	797.9275	25	638.8911
45	513.2681	27	459.2271	61	851.0831	21	728.8167	46	377.6810

Tab. 9: SCs optimum location and sizing.

Fuzzy PSO		Fuzzy ABC		Fuzzy GWO		Fuzzy RAO-1		Fuzzy RAO-3	
SC Node location	SC sizing (kVar)								
50	267.0198	48	493.5362	43	388.2457	61	441.8827	27	287.9169
61	351.9917	61	353.1125	58	363.0878	57	122.4775	60	514.4220
11	414.3575	51	206.4988	55	295.7983	28	449.6673	16	195.6782

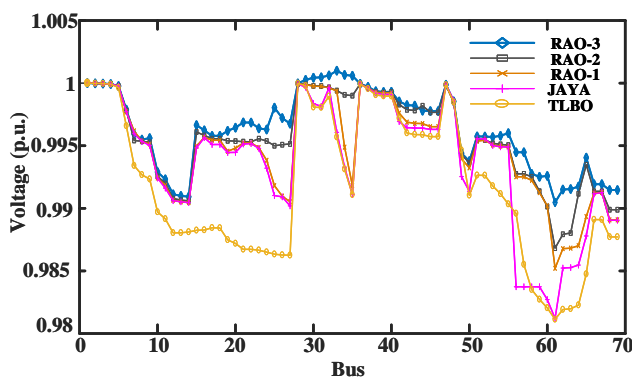


Fig. 9: Voltage curve.

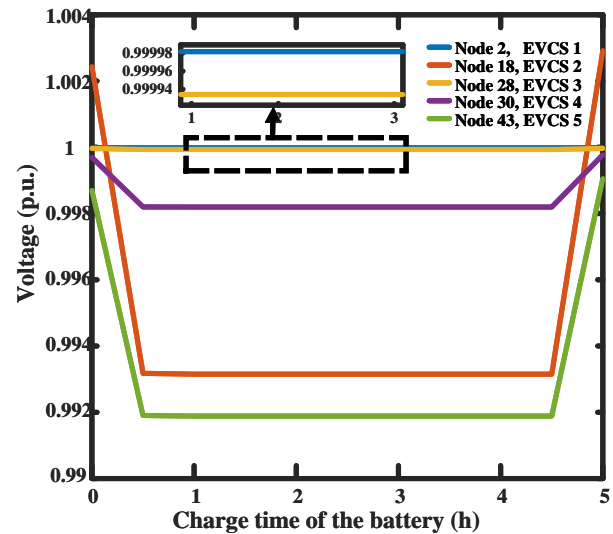


Fig. 11: EVCS Voltage transients.

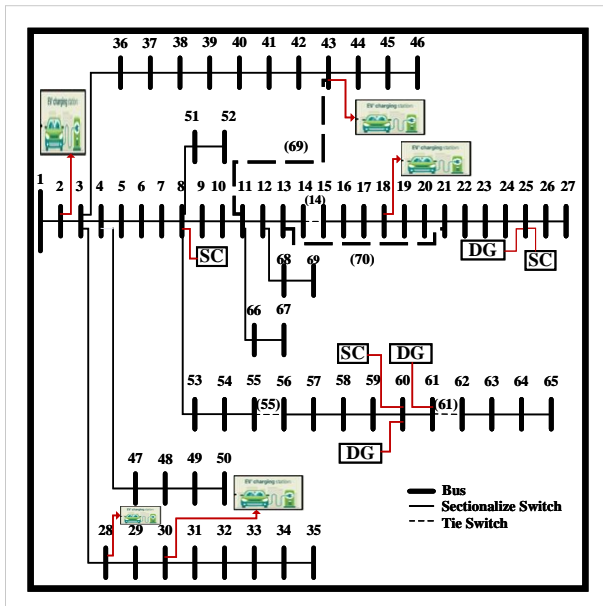


Fig. 10: EVCS, DGs, and SCs allocation in the optimal network structure after reconfiguration.

bus's minimum voltage is enhanced to 0.9905 p.u. and 0.9762 p.u. in scenarios 2 and 1. Compared to the two-stage methodology [17] and scenario 1, the optimal number of EVs in scenario 2 increases to 12.1 % and 10.362 %.

Figure 11 depicts the impact of EVs on EVCS node voltages. It is also worth noting that, even with EV charging demand, the voltage quality may be maintained at kept at deservedly high levels due to the availability of the complete DGs capacity and SCs installations.

Tab. 10: Comparison results.

Cases	Real Power loss (kW)	Minimum Voltage (p.u.)	Total number of EVs
Scenario 2	18.0884	0.9905	213
Scenario 1	39.3467	0.9762	193
Two-stage Methodology [17]	41.01	0.9461	190
Base Case	224.56	0.9092	-

5. Conclusion

This paper suggests an RAO-3 algorithm for 69 bus radial distribution systems with network reconfiguration based on the fuzzy classification technique for the simultaneous optimum size and positioning of EVCS, DGs, and SCs to simultaneously supply the peak of the distribution system and the EV charging load. EV battery charging P and Q load models are built with Li-Ion characteristic curves. The proposed technique achieves its primary goal of (a) reducing active power loss, (b) enhancing the substation power factor, (c) boosting the distribution system's voltage profile, and (d) deploying the optimum number of EVs to EVCS. The influence of transient battery charging load impacts node voltages at the EVCS, and with the help of DGs and SCs, node voltages are kept at acceptable levels during steady-state charging. The existing work can be enhanced with vehicle-to-grid technologies.

Author Contributions

A.K.M. performed writing, original draft, methodology and conceptualisation. S.B.P. performed review and editing.

References

- [1] KALAMBE, S. and G. AGNIHOTRI. Loss minimization techniques used in distribution network: bibliographical survey. *Renewable and Sustainable Energy Reviews*. 2014, vol. 29, iss. 1, pp. 184–200. ISSN 1879-0690. DOI: 10.1016/j.rser.2013.08.075.
- [2] AHMADI, A., A. TAVAKOLI, P. JAMBOR-SALAMATI, N. REZAEI, M. R. MIVEH, F. H. GANDOMAN, A. HEIDARI and A. E. NEZHAD. Power quality improvement in smart grids using electric vehicles: a review. *IET Electrical Systems in Transportation*. 2019, vol. 9, iss. 1, pp. 53–64. ISSN 2042-9746. DOI: 10.1049/iet-est.2018.5023.
- [3] KARMAKER, A. K., S. ROY and M. R. AHMED. Analysis of the Impact of Electric Vehicle Charging Station on Power Quality Issues. In: *2019 International Conference on Electrical, Computer and Communication Engineering (ECCE)*. Coxs-Bazar: IEEE, 2019. pp. 1–6. ISBN 978-1-5386-9111-3. DOI: 10.1109/ECACE.2019.8679164.
- [4] DEB, S., K. KARUNA and P. MAHANTA. Impact of electric vehicle charging stations on reliability of distribution network In: *International Conference on Technological Advancements in Power and Energy (TAP Energy)*. Kollam: IEEE, 2017. pp. 1–6. ISBN 978-1-5386-4021-0. DOI: 10.1109/TAPENERGY.2017.8397272.
- [5] PAWELEK, R., K. PAWEL and I. WASIAK. Experimental analysis of DC electric vehicles charging station operation and its impact on the supplying grid. In: *IEEE International Electric Vehicle Conference (IEVC)*. Florence: IEEE, 2014. pp. 1–5. ISBN 978-1-4799-6075-0. DOI: 10.1109/IEVC.2014.7056152.
- [6] CHEN, L., C. XU, H. SONG and K. JERM-SITTIPARSERT. Optimal sizing and sitting of EVCS in the distribution system using meta-heuristics: A case study. *Energy Reports*. 2021, vol. 7, iss. 1, pp. 208–217. ISSN 2352-4847. DOI: 10.1016/j.egy.2020.12.032.
- [7] LIU, Z, F. WEN and G. LEDWICH. Optimal Planning of Electric-Vehicle Charging Stations in Distribution Systems. *IEEE Transactions on Power Delivery*. 2013, vol. 28, iss. 1, pp. 102–110. ISSN 1937-4208. DOI: 10.1109/TPWRD.2012.2223489.
- [8] AWASTHI, A., K. VENKITUSAMY, S. PADMANABAN, R. SELVAMUTHUKUMARAN, F. BLAABJERG, A. K. SINGH. Optimal planning of electric vehicle charging station at the distribution system using hybrid optimization algorithm. *Energy*. 2017, vol. 133, iss. 1, pp. 70–80. ISSN 1873-6785. DOI: 10.1016/j.energy.2017.05.094.

- [9] GOLLA, N. K. and S. K. SUDABATTULA. WITHDRAWN: Impact of Plug-in electric vehicles on grid integration with distributed energy resources: A comprehensive review on methodology of power interaction and scheduling. *Materials Today: Proceedings*. 2021, vol. 133, iss. 1, pp. 1. ISSN 2214-7853. DOI: 10.1016/j.matpr.2021.03.306.
- [10] RAO, R. S., K. RAVINDRA, K. SATISH and S. V. L. NARASIMHAM. Power Loss Minimization in Distribution System Using Network Reconfiguration in the Presence of Distributed Generation. *IEEE Transactions on Power Systems*. 2013, vol. 28, iss. 1, pp. 317–325. ISSN 1558-0679. DOI: 10.1109/TPWRS.2012.2197227.
- [11] SAVIER, J. S. and D. DAS. Impact of Network Reconfiguration on Loss Allocation of Radial Distribution Systems. *IEEE Transactions on Power Delivery*. 2007, vol. 22, iss. 4, pp. 2473–2480. ISSN 1937-4208. DOI: 10.1109/TPWRD.2007.905370.
- [12] SALKUTY, S. R. Network Reconfiguration of Distribution System with Distributed Generation, Shunt Capacitors and Electric Vehicle Charging Stations. In: *Next Generation Smart Grids: Modeling, Control and Optimization*. 1st ed. Springer: Singapore, 2022, pp. 355–375. ISBN 978-981-16-7794-6. DOI: 10.1007/978-981-16-7794-6.
- [13] KEIN, L. C., T. T. NGUYEN, T. M. PHAN, T. T. NGUYEN. Maximize the penetration level of photovoltaic systems and shunt capacitors in distribution systems for reducing active power loss and eliminating conventional power source. *Sustainable Energy Technologies and Assessments*. 2022, vol. 52, iss. 4, pp. 1–21. ISSN 2213-1396. DOI: 10.1016/j.seta.2022.102253.
- [14] KASTURI, K., C. K. NAYAK, S. PATNAIK, M. R. NAYAK. Strategic integration of photovoltaic, battery energy storage and switchable capacitor for multi-objective optimization of low voltage electricity grid: Assessing grid benefits. *Renewable Energy Focus*. 2022, vol. 41, iss. 1, pp. 104–117. ISSN 1878-0229. DOI: 10.1016/j.ref.2022.02.006.
- [15] SHAHEEN, A. M., A. M. ELSAYED, A. R. GINIDI, R. A. EL-SEHIEMY, E. ELATTAR. A heap-based algorithm with deeper exploitative feature for optimal allocations of distributed generations with feeder reconfiguration in power distribution networks. *Knowledge-Based Systems*. 2022, vol. 241, iss. 1, pp. 1–22. ISSN 1872-7409. DOI: 10.1016/j.knosys.2022.108269.
- [16] LI, L.-L., J.-L. XIONG, M.-L. TSENG, Z. YAN, M. K. LIM. Using multi-objective sparrow search algorithm to establish active distribution network dynamic reconfiguration integrated optimization. *Expert Systems with Applications*. 2022, vol. 193, iss. 1, pp. 1–18. ISSN 1873-6793. DOI: 10.1016/j.eswa.2021.116445.
- [17] GAMPA, S. R., G. PREETHAM, D. DAS and R. BANSAL. Grasshopper optimization algorithm based two stage fuzzy multiobjective approach for optimum sizing and placement of distributed generations, shunt capacitors and electric vehicle charging stations. *Journal of Energy Storage*. 2020, vol. 27, iss. 1, pp. 1–13. ISSN 2352-1538. DOI: 10.1016/j.est.2019.101117.
- [18] SAFARI, A., F. BABAEI and M. FARROKHIFAR. A load frequency control using a PSO-based ANN for micro-grids in the presence of electric vehicles. *International Journal of Ambient Energy*. 2021, vol. 42, iss. 6, pp. 688–700. ISSN 0143-0750. DOI: 10.1080/01430750.2018.1563811.
- [19] MOHANTY, A. and P. S. BABU. Optimal Placement of Electric Vehicle Charging Stations Using JAYA Algorithm. In: *Recent Advances in Power Systems*. 1st ed. Springer: Singapore, 2021, pp. 259–266. ISBN 978-981-15-7993-6. DOI: 10.1007/978-981-15-7994-3_23.
- [20] MOHANTY, A. K. and P. S. BABU. Multi Objective Optimal Planning of Fast Charging station and Distributed Generators in a Distribution System. In: *2021 IEEE 2nd International Conference On Electrical Power and Energy Systems (ICEPES)*. Bhopal: IEEE, 2022, pp. 1–6. ISBN 978-1-6654-0236-1. DOI: 10.1109/ICEPES52894.2021.9699774.
- [21] RAO, R. V. Rao algorithms: Three metaphorless simple algorithms for solving optimization problems. *International Journal of Industrial Engineering Computations*. 2020, vol. 11, iss. 1, pp. 107–130. ISSN 1923-2926. DOI: 10.5267/j.ijiec.2019.6.002.
- [22] QIAN, K., C. ZHOU M. ALLAN and Y. YUAN. Modeling of Load Demand Due to EV Battery Charging in Distribution Systems. *IEEE Transactions on Power Systems*. 2011, vol. 26, iss. 2, pp. 802–810. ISSN 1558-0679. DOI: 10.1109/TPWRS.2010.2057456.
- [23] MASOUM, A. S., S. DEILAMI, P. S. MOSES and A. ABU-SIADA. Impacts of battery charging rates of plug-in electric vehicle on smart grid

distribution systems. In: *2010 IEEE PES Innovative Smart Grid Technologies Conference Europe (ISGT Europe)*. Gothenburg: IEEE, 2010, pp. 1–6. ISBN 978-1-4244-8509-3. DOI: 10.1109/ISGTEUROPE.2010.5638981.

[24] CHAKRAVORTY, M. and D. DAS. Voltage stability analysis of radial distribution networks. *International Journal of Electrical Power & Energy Systems*. 2001, vol. 23, iss. 2, pp. 129–135. ISSN 1879-3517. DOI: 10.1016/S0142-0615(00)00040-5.

[25] DAS, D., H. S. NAGI and D. P. KOTHARI. Novel method for solving radial distribution networks. *IEE Proceedings-Generation, Transmission and Distribution*. 1994, vol. 141, iss. 4, pp. 291–298. ISSN 1359-7051. DOI: 10.1049/ip-gtd:19949966.

About Authors

Ajit Kumar MOHANTY (corresponding author) received his M.Tech. from National Institute of Technology, Trichy in 2013. Currently he is research scholar in the Department of Electrical Engineering, National Institute of Technology, Warangal, India. His research interests include Optimal placement of Electric Vehicles Charging Stations, DGs and Battery modelling.

Suresh Babu PERLI received his Ph.D. from JNTU Hyderabad in year 2011. He is currently working as Associate Professor in the Department of Electrical Engineering, National Institute of Technology, Warangal, India. He has good academic and research experience. His research areas of interest are Optimal placement of charging stations, EVs battery modelling, Power system protections, Optimal PMU placement.